

Ultrafast Terahertz Photoconductivity of Bulk Heterojunction Materials Reveals High Carrier Mobility up to Nanosecond Time Scale

Carlito S. Ponseca, Jr.,[†] Arkady Yartsev,[†] Ergang Wang,^{||} Mats R. Andersson,^{||} Dimali Vithanage,[†] and Villy Sundström^{*†}

[†]Division of Chemical Physics, Lund University, Box 124, 221 00 Lund, Sweden

^{||}Department of Chemical and Biological Engineering/Polymer Technology, Chalmers University of Technology, 412 96 Göteborg, Sweden

ABSTRACT: The few-picosecond (ps) decay of terahertz (THz) photoconductivity typically observed for conjugated polymer:fullerene blends (at excitation fluencies $\sim 10^{15}$ photons/cm² per pulse) is shown to be a result of charge pair annihilation for two polymer:PCBM blends. At a factor of 100 lower excitation density, the THz decay is in the hundreds of ps time scale, implying that very high carrier mobility (~ 0.1 cm² V⁻¹ s⁻¹) prevails for long time after charge formation, of importance for free charge formation in organic solar cells.

Time resolved terahertz (THz)^{1–4} and microwave^{5,6} spectroscopies have been used in probing charge carrier dynamics in both organic and inorganic solar cell materials. Several recent papers reported the generation, relaxation, and recombination of photoexcited species in several polymer:PCBM ([6,6]-phenyl-C61-butyric acid methyl ester) systems using time-resolved terahertz spectroscopy (TRTS).^{7–9} The wide use of this technique is primarily due to its noncontact nature, resolution in the subpicosecond (sub-ps) time domain, and its sensitivity to carrier mobilities. In the commonly observed THz dynamics of polymer:PCBM thin films, photogenerated species are created almost instantaneously after photoexcitation followed by a ps decay and a much slower low amplitude nanosecond (ns) lifetime of carriers. Ai et al. measured the photoconductivity of poly(3-hexylthiophene) (P3HT) blended with PCBM in different weight concentrations.² The dynamics show fast rise, fast decay, and then a slower decay in hundreds of ps. The subsequent pump power dependence measurement showed that the early time decay becomes faster and more dominant with increasing fluence. The response was assigned to either exciton–exciton annihilation, interfacial charge transfer, and/or competition between them depending on the concentration of PCBM. Esenturk et al., on the other hand, showed that the effect of adding PCBM electron traps to P3HT resulted in changes in the peak and long time response but would not lead to changes in the fast decay.⁷ This was supported by the work of Cunningham et al. where excitation of the blends below or above its band gap did not affect the dynamics of the initial decay but the peak THz response only.⁸ Two other types of polymers, APFO-3 and LBPP-1, blended with PCBM were studied using TRTS.^{9,10} In the case of LBPP-1, the few ps fast decay was surmised as cooling of highly mobile charges that are initially able to pass over potential barriers and as they cool

down the barriers limits the motion. The transition from the hot regime to a quasi-equilibrium state was suggested to be not more than 2 ps.¹⁰ For APFO-3:PCBM, the effect of two different excitation fluencies showed the initial decay speeding up at higher pump power. This dependence was then related to the calculated amplitude of the concentration-mobility product showing the lifetime of the coupled polaron pair.⁹ In all of the reported works mentioned above, a very similar THz response decay was observed for the first 10 ps (see Figure 1), despite

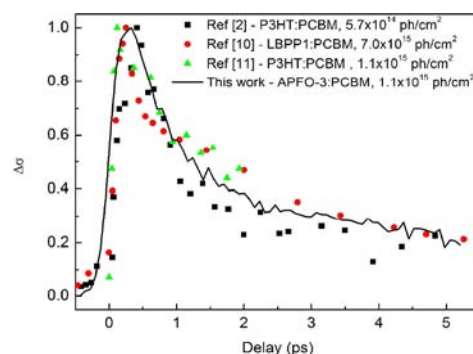


Figure 1. Normalized transient conductivity kinetics of APFO-3poly:PCBM and several other polymer:PCBM blends from literature. Data points from refs 10, 11 were adapted with permission. Copyrighted 2009, 2011 by the American Physical Society.

quite different polymer:PCBM blends. It is important to note that though TRTS is a powerful tool in probing carrier dynamics on this time scale, high excitation densities are routinely used to ensure that enough charge carriers are photoexcited in order to extract a decent signal. However, at such high fluence conditions, the dynamics of carriers may be altered. In particular, transient absorption spectroscopy with probe in the visible to near-infrared domain on APFO-3:PCBM at low excitation fluence hints that such hypothesis cannot be ruled out.¹²

In this communication, ultrafast THz dynamics of carriers is investigated by varying the excitation light intensity by at least two orders. We focus on the early ps decay dynamics and its dependence on high density excitation. Two polymers TQ1 [2,3-bis-(3-octyloxyphenyl)quinoxaline-5,8-diyl-*alt*-thiophene-2,5-diyl]¹³ and APFO-3 poly([2,7-(9,9-dioctyl-fluorene)-*alt*-5,5-

Received: February 22, 2012

Published: July 2, 2012

(4',7'-di-2-thienyl-2',1',3-benzothiadiazole)]¹⁴ blended with the PCBM electron acceptor were studied. Both showed excitation fluence dependence of the early time, 1–10 ps decay. At lower pump power ($\sim 10^{12}$ – 10^{13} photons/cm² per pulse), the decay of transient photoconductivity, that is, the polaron pair concentration mobility product, was estimated to be in the hundreds of ps, while at high fluence and thus high charge density ($\sim 10^{14}$ – 10^{15} photons/cm² per pulse), the conductivity decays in several ps due to polaron pair annihilation.

Polymers of TQ1 ($M_n = 49\,000$, $M_w = 153\,000$ g/mol) and APFO-3 ($M_n = 4900$, $M_w = 11\,800$ g/mol) were blended with commercially available PCBM at 1:2 and 1:4 weight ratio, respectively. The weight ratios were chosen in order to obtain the highest THz response and also have the highest solar cell efficiency. The solution was drop-cast on a quartz silica glass and dried in open environment. An encapsulated 100 nm thin film prepared in an inert atmosphere was used for transient absorption measurements of TQ1:PCBM.

The THz photoconductivity spectrum was determined using a TRTS setup similar to that used in ref 15. In our case, however, we used 580 and 610 nm pulses for the photo-excitation of APFO-3 and TQ1, respectively. The photon flux was varied from 1.8×10^{15} to 9.1×10^{12} photons/cm² per pulse by using neutral density filters. Analysis of the transient transmittance to obtain THz photoconductivity of the samples is described in detail in refs 15 and 16. The result of these measurements is primarily the photoconductivity spectrum $\Delta\sigma$ normalized by the density of excited charges $e_0 n_{\text{exc}}$ which corresponds to the product of the quantum yield of the excitation ξ and its mobility spectrum μ :

$$\frac{\Delta\sigma}{e_0 n_{\text{exc}}} = \xi \cdot \mu \quad (1)$$

Transient photoconductivity spectra of TQ1 extracted using the high (1.8×10^{15} photons/cm² per pulse) and low (9.1×10^{12} photons/cm² per pulse) excitation densities at three representative time delays are shown in Figure 2. For both

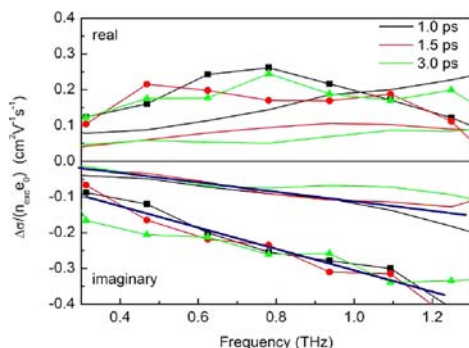


Figure 2. Transient mobility spectra of TQ1 obtained from excitation densities of 1.8×10^{15} photons/cm² per pulse (lines) and 9.1×10^{12} photons/cm² per pulse (lines with symbols). Blue line is for clarity of the dependence of imaginary part.

excitation densities, a dependence on frequency was observed with positive real and negative imaginary parts increasing. Confined transport of photoexcited species are commonly characterized by such behavior.^{8,17,18} Using this signature, one can assign the nature of the photogenerated species. A tightly bound exciton would manifest by a zero real part, since the absorption resonance of the excited state exciton is far from

THz frequencies. Contribution from polymer excitons to the THz response can be also excluded because they are very efficiently quenched by the charge generation and do not exist beyond ~ 200 fs^{12,19} (see also TA kinetics of TQ1:PCBM in inset Figure 3a, showing ultrafast formation of charges). On the

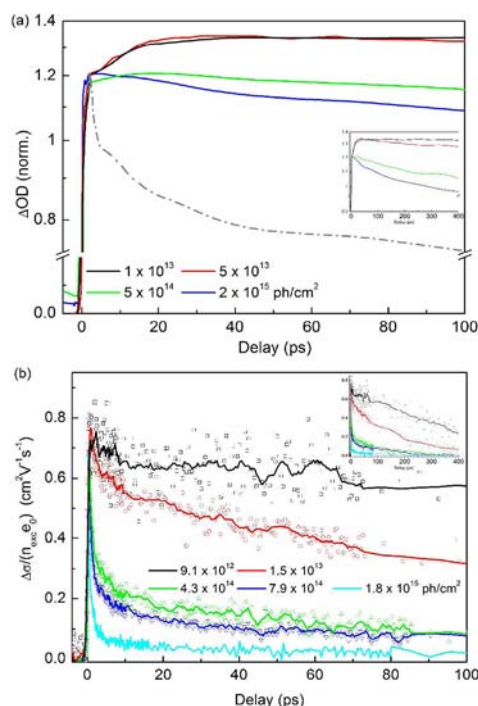


Figure 3. (a) Transient absorption and (b) transient THz conductivity kinetics of TQ1:PCBM at varying excitation densities. Insets are plots for longer pump–probe delay times. The difference between the highest and lowest intensity in TA kinetics is shown as broken line. Lines in the THz kinetics are smoothed data for clarity of the plot except for highest excitation fluence.

other hand, free charge carriers induce strong absorption in the THz electric field yielding a non-zero value of the real part of conductivity.² The measured conductivity spectra in this work has non-zero real part, that is, free charge carrier-like and has an imaginary part which is negatively increasing reaching zero at the lowest frequency, that is, exciton-like. The photoexcited species observed here, therefore, should be charged and at the same time Coulombically (loosely) bound. In the previous TRTS measurements of APFO-3:PCBM, a similar shape of the conductivity spectrum was obtained and assigned to coupled polaron pairs using the calculated time dependent amplitude of the mobility.⁹ We therefore conclude that the primary photoproduct detected here by TRTS on this time scale is a loosely coupled polaron pair for both APFO-3:PCBM and TQ1:PCBM. We note that in the work of Nemeč et al., on APFO-3:PCBM, this loosely coupled polaron pair has an initial high mobility¹⁰ and a separation distance of ~ 4 nm, as estimated by Pal et al.¹⁹

Comparing the conductivity spectra normalized for excitation density ($\Delta\sigma/(n_{\text{exc}}e_0)$, Figure 2) at two excitation densities, we can see that lower excitation density results in apparently higher normalized spectral response for both the real and imaginary parts of the conductivity spectrum; for the imaginary part, the effect is quite clear, but for the real part somewhat obscured by a larger noise in the measured spectra. The amplitudes of both real and imaginary parts of the conductivity spectra depend on

the number of photogenerated charges as expressed in eq 1. If the decay of charge population is significantly slower than the temporal resolution of the experiment, we expect a linear relationship between spectral amplitudes and excitation density; the normalized spectra in Figure 2 should in this case all be identical. If, on the other hand, there is a very fast process, on the order of the temporal resolution of the experiment reducing the charge density, then spectra measured at early and late times may have different amplitudes since some decay of charge density will occur already during the temporal response function. Inspection of the spectra in Figure 2 shows that the spectral amplitudes of both the real and imaginary parts are larger at lower excitation density, precisely the dependence we expect if there is an ultrafast unresolved decay of charge carrier density at high excitation intensities. Below we will show that the same conclusion can be drawn from the conductivity kinetics, and the explanation can be found in previous TA measurements of charge pair generation and recombination in the studied materials.^{12,19}

Transient absorption measurements in the optical and near-infrared spectral domains on APFO-3:PCBM thin film blends show that at low excitation density ($\sim 10^{13}$ photons/cm² per pulse) charge carrier recombination occurs on the many ns and even slower time scale as a result of geminate and nongeminate electron–hole recombination. At high excitation densities ($\sim 10^{15}$ photons/cm² per pulse), a very fast, few-ps decay of charge carrier population was observed and interpreted as “polaron pair annihilation”.^{12,19} The rationale behind this interpretation is that at these high excitation densities the distance between photogenerated charge pairs is so small (~ 4 nm) that very little charge diffusion is required for recombination, that is, nonequilibrated charge pairs recombine or “annihilate” immediately after their formation. This charge annihilation process could be described as an excitation intensity dependent decay of charge carrier concentration on the few-ps time scale, faster at higher intensity.¹² The TA kinetics of TQ1:PCBM has very similar dynamics as shown in Figure 3a; a resolution limited rise reflects charge generation, and at the lowest intensities, there is an ~ 10 ps rise in the kinetics due to charge separation (similar to APFO-3:PCBM^{12,19}) and very slow ns decay. At high intensity, this rise is canceled by the fast decay due to the polaron pair annihilation. To visualize the time dependence of this annihilation, the difference between a lowest and highest intensity trace is plotted in Figure 3a (broken line).

Time resolved THz kinetics of TQ1:PCBM at varying excitation densities are shown in Figure 3b. At the lowest intensity, the kinetics does not decay up to 100 ps, similar to the TA kinetics in Figure 3a. As the excitation fluence is increased, increasing amplitudes of few-ps decays become apparent, very similar to the fast TA decays at high intensity (Figure 3a). For both THz and TA, at the highest intensities, $\sim 50\%$ of the fast decay occurs in ~ 5 ps and after ~ 30 ps both are down to the long time background level. At low intensity, for the hundreds of ps to ns time scale, the TA kinetics still remain constant while the THz kinetics decay to half of its initial signal (insets in Figure 3b). From eq 1, we know that the photoinduced THz signal is a product of charge yield and mobility. TA kinetics of TQ1:PCBM show that the charge concentration is constant up to the ns time scale, implying that the THz kinetics reflect the decay of mobility alone, possibly due to charge carrier cooling and trapping.⁹

For comparison, Figure 4 shows plots of the THz transient conductivity kinetics for APFO-3:PCBM at two different

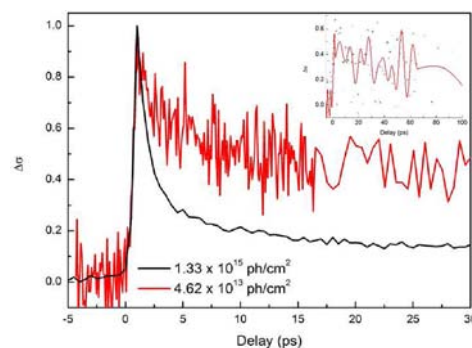


Figure 4. THz transient conductivity kinetics of APFO-3:PCBM at two excitation densities normalized to unity. Inset shows an attempt to measure APFO-3:PCBM at even lower excitation density, 2.0×10^{13} photons/cm² per pulse. The decay appears to be even longer, but here the signal-to-noise is large due to a very weak signal (the line represents smoothing of data).

excitation densities. Because of the approximately factor of 5 higher mobility in the TQ1:PCBM blend as compared to APFO-3:PCBM (see ref 20 for mobility spectra of APFO-3:PCBM), TQ1:PCBM could be measured down to lower excitation density and with considerably better signal-to-noise. For both polymers, an apparatus response limited ultrafast rise in the THz photoconductivity is observed for all pump conditions, reflecting the efficient formation of coupled polaron pairs. This also means that exciton diffusion through extended polymer domains can be ruled out since this would manifest as a slow rise in the THz kinetics. The same conclusion was obtained from measurements of fluorescence quenching of APFO-3:PCBM (discussed in detail in refs 12 and 19) and TQ1:PCBM (not shown), as well as TA measurements of charge generation (refs 12, 19, 20, for APFO-3:PCBM and Figure 3a for TQ1:PCBM).

As illustrated by the THz kinetics in Figures 3b and 4, both polymer:PCBM blends exhibit an excitation density dependent ultrafast decay of the THz response. At the longest time delay (>350 ps), we observe a low amplitude long-lived signal decaying on the many hundreds of ps to ns time scale. Most if not all of the published works on bulk heterojunction materials (BHJ) that used TRTS has obtained very similar kinetics. These are plotted in Figure 1 where the pump fluence used is also shown. The fast decay has been previously explained as charge carrier cooling,^{8,9} self-localization, and formation of excitons.¹¹ According to Ai et al., depending on P3HT:PCBM ratio, the early time (~ 1 ps) can be due to exciton–exciton annihilation, interfacial charge transfer, and/or competition between them. They further suggested that at later time delays (~ 75 ps), the dependence on pump fluence has a different origin, assigned to second-order recombination, for example, recombination of electrons in PCBM and holes in P3HT. The strong fluence dependence of the decay rate on this time scale agrees, both in the time scale on which it occurs and the excitation density for which it is observed, with the charge pair annihilation discussed above for TA kinetics of APFO-3:PCBM¹² and TQ1:PCBM (compare TA decay in Figure 3a (broken line) and THz decays at high intensity in Figure 3b). We therefore assign the fast few-ps time scale decay of the THz photoconductivity signal observed here to this charge pair

annihilation process. It should be mentioned that, although there have been previous studies on APFO-3:PCBM using TRTS,⁹ the excitation intensity dependence of the THz conductivity was not observed; the 5 times smaller mobility in APFO-3:PCBM²⁰ than TQ1:PCBM results in a very small THz response, which at that time made it impossible to perform measurements at sufficiently low intensities to eliminate the charge pair annihilation process. Here it is also important to point out that exciton–exciton annihilation within the polymer, prior to charge pair generation, can be excluded as a mechanism for the intensity dependent THz conductivity decay. The reason is that such exciton annihilation relies on energy transfer along the polymer chains, which occurs on the few-ps time scale and longer,²¹ but because of the very fast ~100 fs charge generation, all excited states have been depleted before any energy transfer and exciton annihilation can occur.

At low enough excitation density ($\sim 10^{12}$ – 10^{13} photons/cm² per pulse), that is, fewer photoexcited carriers, the ps-decay of the THz response can be almost eliminated. The geminate and nongeminate electron–hole recombination of mobile charges observed at such carrier densities in optical and near-IR transient absorption measurements on these materials are characterized by nonexponential decays carrying decay components ranging from hundreds of ps to ns and microseconds (μ s), depending on the exact density of charge carriers and the interplay between geminate and nongeminate electron–hole recombination (refs 12 and 19, for APFO-3:PCBM and Figure 3a for TQ1:PCBM). As already mentioned above, the slow hundreds of ps THz conductivity decays we observe (Figures 3b and 4) for both materials at the lowest intensities attainable in the present experiments are similar, but still faster than the rates of charge recombination observed in optical transient absorption experiments at similar excitation densities (refs 12, 19, and Figure 3a). This can be understood as a result of the THz decay not being limited by the decay of carrier population, but by the decay of carrier mobility. Such high carrier mobility was also reported in refs 5 and 6, and for microcrystalline powder PCBM²² and P3HT:PCBM²³ film blends where it extends up to many ns and μ s time scales.

We have shown that the ubiquitously observed ps time scale decay of THz conductivity in BHJ conjugated polymer:fullerene blends is a result of ultrafast charge pair annihilation occurring at the high carrier densities resulting from high excitation pulse intensities generally used in time-resolved THz measurements. When reducing the excitation fluence to $< 10^{13}$ photons/cm² per pulse, the very fast THz conductivity decay can be almost entirely eliminated and the THz decay is now in the hundreds of ps to ns time scale and not limited by the decay of carrier population, but by the actual decay of carrier mobility. Thus, the present measurements also show that carrier cooling and trapping in these materials occur on the hundreds of ps and ns time scale, much slower than previously reported.^{8,9,19} This implies that the photogenerated charges maintain a very high mobility (~ 0.1 cm² V⁻¹ s⁻¹) for hundreds of ps, which of course has far reaching implications for how photogenerated charges separate and form free mobile charges that can be extracted as photocurrent in a functioning solar cell.

AUTHOR INFORMATION

Corresponding Author

villy.sundstrom@chemphys.lu.se

Notes

The authors declare no competing financial interest.

ACKNOWLEDGMENTS

The Swedish Energy Agency (STEM), the Swedish Research Council, the Knut&Alice Wallenberg foundation and the European Research Council (Advanced Investigator Grant to V.S., 226136-VISCHEM) are acknowledged. Zhoquiang Wang is also acknowledged for the preparation of the TQ1:PCBM thin film used for transient absorption measurements.

REFERENCES

- (1) Parkinson, P.; Lloyd-Hughes, J.; Johnston, M. B.; Herz, L. M. *Phys. Rev. B* **2008**, *78*, 115321.
- (2) Ai, X.; Beard, M. C.; Knutsen, K. P.; Shaheen, S. E.; Rumbles, G.; Ellingson, R. J. *J. Phys. Chem. B* **2006**, *110*, 25462.
- (3) Němec, H.; Kužel, P.; Sundström, V. *J. Photochem. Photobiol.* **2010**, *A215*, 123.
- (4) Esenturk, O.; Melinger, J. S.; Heilweil, E. J. *J. Appl. Phys.* **2008**, *103*, 023102.
- (5) Grzegorzczak, W. J.; Savenije, T. J.; Dykstra, T. E.; Piris, J.; Schins, J. M.; Siebbeles, L. D. A. *J. Phys. Chem. C* **2010**, *114*, 5182.
- (6) Ferguson, A. J.; Kopidakis, N.; Shaheen, S. E.; Rumbles, G. *J. Phys. Chem. C* **2011**, *115*, 23134.
- (7) Esenturk, O.; Melinger, J. S.; Heilweil, E. J. *J. Appl. Phys.* **2008**, *103*, 023102.
- (8) Cunningham, P. D.; Hayden, L. M. *J. Phys. Chem. C* **2008**, *112*, 7928.
- (9) Němec, H.; Nienhuys, H. K.; Zhang, F.; Inganäs, O.; Yartsev, A.; Sundström, V. *J. Phys. Chem. C* **2008**, *112*, 6558.
- (10) Němec, H.; Nienhuys, H.-K.; Perzon, E.; Zhang, F.; Inganäs, O.; Kužel, P.; Sundström, V. *Phys. Rev. B* **2009**, *79*, 245326.
- (11) Cooke, D. G.; Krebs, F. C.; Jepsen, P. U. *Phys. Rev. Lett.* **2011**, *108*, 056603.
- (12) De, S.; Pascher, T.; Maiti, M.; Jespersen, K. G.; Kesti, T.; Zhang, F.; Inganäs, O.; Yartsev, A.; Sundstrom, V. *J. Am. Chem. Soc.* **2007**, *129*, 8466.
- (13) Wang, E.; Hou, L.; Wang, Z.; Hellström, S.; Zhang, F.; Inganäs, O.; Andersson, M. R. *Adv. Mater.* **2010**, *22*, 5240.
- (14) Svensson, M.; Zhang, F.; Veenstra, S. C.; Verhees, W. J. H.; Hummelen, J. C.; Kroon, J. M.; Inganäs, O.; Andersson, M. R. *Adv. Mater.* **2003**, *15*, 988.
- (15) Němec, H.; Nienhuys, H.-K.; Perzon, E.; Zhang, F.; Inganäs, O.; Kužel, P.; Sundström, V. *Phys. Rev. B* **2009**, *79*, 245326.
- (16) Ulbricht, R.; Hendry, E.; Shan, J.; Heinz, T. F.; Bonn, M. *Rev. Mod. Phys.* **2011**, *83*, 543.
- (17) Hendry, E.; Koeberg, M.; Schins, J. M.; Nienhuys, H. K.; Sundstrom, V.; Siebbeles, L. D. A.; Bonn, M. *Phys. Rev. B* **2005**, *71*, 125201.
- (18) Papathanassiou, A. N.; Sakellis, I.; Grammatikakis, J. *J. Appl. Phys. Lett.* **2007**, *91*, 122911.
- (19) Pal, S. K.; Kesti, T.; Maiti, M.; Zhang, F.; Inganäs, O.; Hellström, S.; Andersson, M. R.; Oswald, F.; Langa, F.; Österman, T.; Pascher, T.; Yartsev, A.; Sundström, V. *J. Am. Chem. Soc.* **2010**, *132*, 12440.
- (20) Ponseca, C. S., Jr.; Němec, H.; Vukmirović, N.; Fusco, S.; Andersson, M.; Yartsev, A.; Sundström, V. *J. Am. Chem. Soc.* **2012**, submitted for publication.
- (21) Scheblykin, I.; Yartsev, A.; Pullerits, T.; Gulbinas, V.; Sundström, V. *J. Phys. Chem. B* **2007**, *111*, 6303.
- (22) de Haas, M. P.; Warman, J. M.; Anthopoulos, T. D.; de Leeuw, D. M. *Adv. Func. Mater. B* **2006**, *16*, 2274.
- (23) Savenije, T. J.; Murthy, D. H. K.; Gunz, M.; Gorenflot, J.; Siebbeles, L. D. A.; Dyakonov, V.; Diebel, C. *J. Phys. Chem. Lett.* **2011**, *2*, 1368.